2-4-2008

Designs and Optical Tests of Thermal Links for an Optical Refrigerator

John Parker

David Mar

Steven Von der Porten

John Hankinson

Kevin Byram

See next page for additional authors

Recommended Citation

Parker, J., D. Mar, S. Von der Porten, J. Hankinson, K. Byram, C. Lee, K. Mayeda, R. Haskell, Q. Yang, S. Greenfield, and R. Epstein. "Designs and optical tests of thermal links for an optical refrigerator." Proceedings from the Laser Refrigeration of Solids SPIE Conference in San Jose California on 23 January 2008. (2008): 69070D.1-69070D.12. DOI: 10.1117/12.764166

Designs and Optical Tests of Thermal Links for an Optical Refrigerator

John Parker*[a], David Mar[a], Steven Von der Porten[a], John Hankinson[a], Kevin Byram[a], Chris Lee[a], Kai Mayeda[a], Richard Haskell[a], Qimin Yang[a], Scott Greenfield[b], Richard Epstein[c]

[a] Departments of Engineering and Physics, Harvey Mudd College, Claremont, CA 91711-3116;
[b] Chemistry Division, Los Alamos National Laboratory, MS J565, Los Alamos, NM 87545;
[c] International Space & Response Division, Los Alamos National Laboratory, MS B244, Los Alamos, NM 87545

ABSTRACT

Dielectric mirror leakage at large angles of incidence limits the effectiveness of solid state optical refrigerators due to reheating caused by photon absorption in an attached load. In this paper, we present several thermally conductive link solutions to greatly reduce the net photon absorption. The Los Alamos Solid State Optical Refrigerator (LASSOR) has demonstrated cooling of a Yb^{3+} doped ZBLANP glass to 208 K. We have designed optically isolating thermal link geometries capable of extending cooling to a typical heat load with minimal absorptive reheating, and we have tested the optical performance of these designs. A surrogate source operating at 625 nm was used to mimic the angular distribution of light from the LASSOR cooling element. While total link performance is dependent on additional factors, we have found that the best thermal link reduced the net transmission of photons to 0.04%, which includes the trapping mirrors 8.1% transmission. Our measurements of the optical performance of the various link geometries are supported by computer simulations of the designs using Code V, a commercially available optical modeling software package.

Keywords: Optical Isolation, Optical Shielding, Optical Refrigeration, Laser Cooling, Optical Cryocooler, Code V, Optical Modeling

1. INTRODUCTION

In the last century a common design task has been the creation of links that confine and propagate light. Yet there are few scenarios that have necessitated a link - that is thermally conductive and optically absorptionless - to prevent the propagation of light. The input to our link is a wide angular distribution of near-isotropic photons over a 1 cm^2 aperture. The desired output is complete optical isolation and transfer absorption must be negligible. Our system functions as thermal link for attaching heat loads to the Los Alamos Solid State Optical Refrigerator (LASSOR). In 2002, Ball Aerospace reported that the angle dependent reflectivity inherent to all dielectric trapping mirrors allowed considerable photon leakage at high angles of incidence preventing the direct attachment of heat loads to the cooler [1]. We report here on several thermal link designs and present, to our knowledge, the lowest recorded optical transmission for a thermal link in publication.

1.1 Laser Cooling Physics

The first cooling results from anti-Stokes fluorescence of Yb^{3+} doped ZBLANP were reported by LASSOR in 1995 [2]. In the anti-Stokes fluorescence process, a pump laser photon is absorbed by a thermally excited dopant ion in the highest level of the ground-manifold [3-4]. The pump photon excites the ion to a higher energy manifold and then relaxes to a lower state in the ground-manifold, releasing a photon of higher energy than the one absorbed - thus cooling the system. The process repeats when thermal phonon energy is absorbed and an ion returns to the top of the ground-manifold.

To takes advantage of this phenomenon to cool, the wavelength of pump laser light has just enough energy to excite a Yb^{3+} dopant ion in the ZBLANP glass from the highest energy level of the ground-manifold to the lowest energy level of the next manifold, thus when the ion relaxes it must release a photon with at least as much energy as the absorbed photon. An important characteristic of this process is that the average energy liberated from the system per excitation-relaxation cycle is much smaller than the energy of the photons involved. As a result, it is crucial to understand where

Laser Refrigeration of Solids, edited by Richard I. Epstein, Mansoor Sheik-Bahae,
Proc. of SPIE Vol. 6907, 69070D, (2008) · 0277-786X/08/$18 · doi: 10.1117/12.764166

the fluoresced photons go after their emission as any absorption of the high-energy fluorescence that results in heating greatly diminishes the net cooling effect of the process.

1.2 Basic Model

In the LASSOR system a near-infrared laser (~1 μm wavelength) is incident on a small 1 cm^3 sample of Yb^{3+} doped ZBLANP glass. The laser beam is confined within the glass by a set of dielectric trapping mirrors causing the beam to be fully absorbed by the Ytterbium ions. The absorption of this laser light causes the glass to re-emit higher energy photons (anti-Stokes fluorescence), resulting in a net energy loss and cooling of the glass. In 1999, the LASSOR team demonstrated a cooling drop of 48 °C without an attached heat load [5]. In 2005, LASSOR reported cooling from room temperature to 208 K using an improved system and a higher power laser [6]. Optical refrigeration using proprietary thermal links to attached heat loads has been reported by Ball Aerospace and a cooling drop of 7.9 °C was demonstrated using a load equivalent in size to a small sensor [7-9].

The basic model for a thermal link is simple. We assume that fluoresced photons originate uniformly throughout the cooling element and are emitted isotropically. To prevent undesirable heating, these photons must be transmitted to the outer chamber wall where their absorption does not affect the cooling process. We refer to these absorptive walls as "baffling" to avoid confusion with other interfaces. A vacuum separates the cooling source from the baffling to prevent convective heat transfer. The system uses 6 to 10 cylindrical fibers with ~ 100 micron diameter to mechanically suspend the cooling element from the baffling.

The cooling efficiency of the system is below 1% at steady-state, consequently the average power of the light fluoresced from the ZBLANP crystal is two orders of magnitude greater than the average power removed from the system in the cooling process. The transfer of this refrigeration effect to a useful thermal load, such as a small processor or focal plane, can be nullified by a few leaked photons. When the high-energy fluoresced photons are absorbed anywhere other than the baffling, heating occurs and the cooling effect is reduced. At room temperature photon absorption is the major source of undesirable heating, while other heating mechanisms become dominant at lower temperatures including conduction from the support fibers and black-body radiation from the baffling [10].

2. THERMAL LINK DESIGN

The dielectric trapping mirrors on the cooling source greatly limit the amount of near-normal incidence light transmitted through that face while allowing off-normal rays to propagate through. As a consequence, link designs must prevent these off-normal rays from reaching the potentially absorptive heat load region.

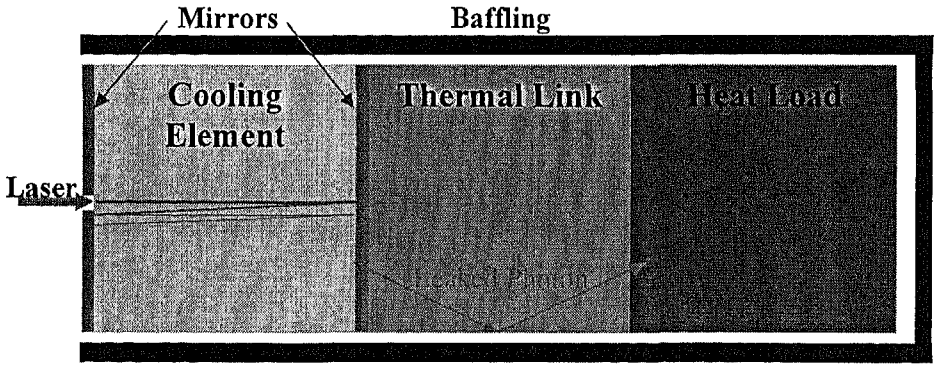

Fig. 1. This figure shows the simplest link design using a block of transparent material. The large arrow on left shows the pump laser light incident on the cooling source. The arrow passing through the trapping mirrors and thermal link shows an example of a leaked light ray that would reflect through the link.

As the figure suggests, if poor link geometry is chosen, fluoresced photons will be guided, via total internal reflection, through the link to the load. We have designed four types of geometric solutions to minimize the transmission of the

photons to the load. The designs focus on reducing the photons leaked through the dielectric mirror, which occurs at angles of incidence >30°. To simplify the initial analysis of these models, we have approximated the Fresnel reflections at the link-vacuum interface as a step function around the critical angle. The transmission of light onto the baffling can be increased by the use of anti-reflective coatings applied at all vacuum interfaces, square cross-sections to minimize lateral modes, and a material with low index of refraction to increase the critical angle. In addition to limiting photon absorption, the surface area of the thermal link must be minimized to reduce heat absorption from the black-body radiation of the baffling, and the cross-sectional area of the link must be large enough to provide good conductive heat transfer between the thermal load and the cooling source. These two factors are not initially dominant but have a greater effect as the temperature drops [10].

2.1 Design 1: Multiple Mirrors

This solution involves using multiple highly reflective coatings in the space between the cooling element and the thermal load in order to reflect light outward onto the baffling. The design is based on the assumption of absorptionless dielectric mirrors which have a high reflectivity envelope over a narrow band of angles. By using multiple mirrors tuned to reflect different angles of incidence, the design prevents light from reaching the load. Fig. 2 shows the simplest case using only two mirrors.

Assuming high reflectivity for a 0° to 30° envelope of incidence angles, we can ensure no light rays have a direct path from the fluorescing face of the cooling source to the absorptive thermal load by separating them by at least 3.5 cm away. As a result, the second mirror will only be responsible for >30° off-normal rays that have been reflected at the link-vacuum interface. For example, having a second mirror tuned to reflect light incident from 30°-60° blocks those leaked rays being guided down the link. The steeper rays from 60°-90° are transmitted out to the baffling as they are below the critical angle on the lateral faces.

Fig. 3 shows a magnified view of the thermal link-vacuum interface at the top of the link in Fig. 2. This figure shows the distinct ranges of angular incidence on the link-vacuum interface. Region A shows angles of incidence on the interface greater than 60°, which theoretically should be of negligible intensity if the first dielectric mirror reflects essentially all of the rays incident upon it with small angles of incidence. Region C shows angles of incidence that will transmit a fraction of the light through the interface to the baffling as the rays are incident upon the interface at angles smaller than the critical angle. Finally, region B shows the angles that will have been passed by the first mirror and fall within the total internal reflection envelope on the lateral interface. It should be noted that at angles only a few degrees smaller than θ_{TIR}, Fresnel reflection will still be high and this part of region C will be reflected back into the thermal link well. It is the light rays in region B and high angles in C that the second mirror is intended to shield from the thermal load.

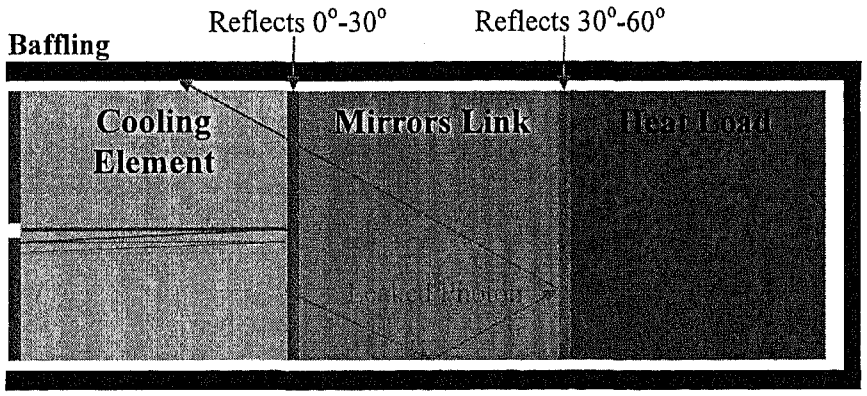

Fig. 2. Multiple cascaded mirrors to reduce leaked light to the load. The mirrors on cooling source have the greatest reflectivity around normal incidence. As the light propagated towards the load the additional mirrors have peak reflectivity at increasing angles of incidence.

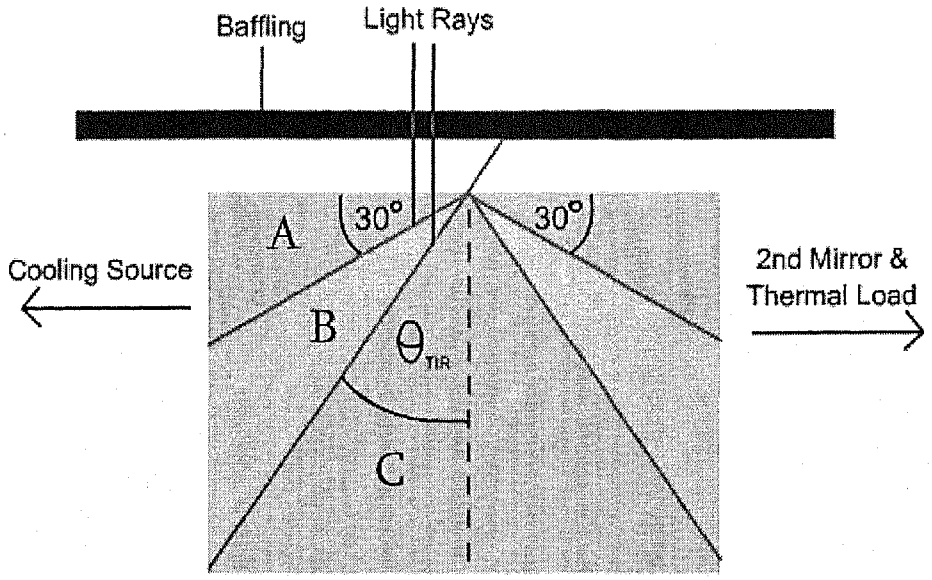

Fig. 3. This figure is a magnified view of the thermal link-to-vacuum interface (top and center of the link in Figure 5). Region A is dark given that the first dielectric mirror has high reflectance from 0°-30° angle of incidence. Region C is dark given the range of angles less than the critical angle (an example of n = 1.75, critical angle = 35° is used here). Region B shows the range of angles that will leak through the first mirror and be totally internally reflected through the thermal link.

The addition of multiple reflection surfaces in the system brings up issues of potentially trapped rays. In this situation, very low absorption levels in the link or mirror coatings could end up generating an unacceptable amount of heat that reverse the cooling process.

2.2 Design 2: Kinked Waveguide

This design utilizes a kinked waveguide structure for the thermal link that places the load off-axis from the cooling element while allowing light to leak out of the link to the baffling, before reaching the load. In a step-index waveguide, light propagates in the fiber through a series of shallow reflections off the sides. The kink in our waveguide causes light, which hits the sides at shallow angles in the first half of the link, to be incident at near-normal angles relative to the sides of the second half of the link. This allows light that was propagating through the waveguide to exit the link material and be absorbed by the baffling. The corner angle φ is varied based on the distribution of light entering the link. When multiple kinks are cascaded, in which each kink has a corner angle tuned to a different distribution of light, the total attenuation of light through the link will further increase.

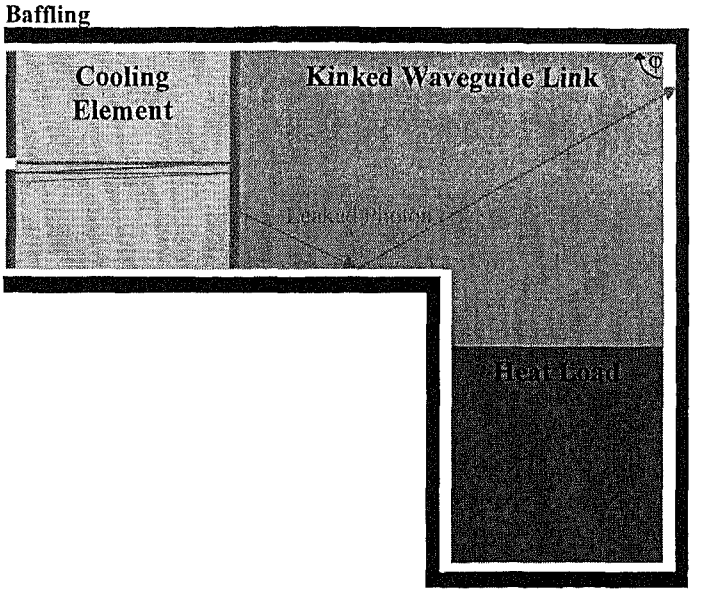

Fig. 4. The high angle kink allows light to leave the thermal link before reaching the load. The arrows within the link represent leaked light rays transmitting through the right-hand face. The corner angle φ is adjusted in order to optimize the design.

2.3 Design 3: Hemisphere

The hemispherical design creates a link-vacuum interface that is near-normal incidence at all points to the cooling element's emitted photons. This is achieved by making a hemisphere with a radius larger than the size of the emitting face. In the limit as the hemisphere grows large, the cooling source effectively becomes a point source and the isotropically emitted photons are incident close to normal on the vacuum interface. Reflections are minimal and the photons are delivered to the surrounding baffling. To minimize link size, the emitted photons are only required to have an angle of incidence less than the critical angle, and as a result the minimum radius of the hemisphere is dependent on the refractive index. This is shown by Equation 1 for a 1 cm by 1 cm emission face with trapping mirrors that are highly reflective up to 30°.

$$r_{\min} = \frac{n_1\sqrt{3}}{4} cm \approx .43\, cm \cdot n_1 \tag{1}$$

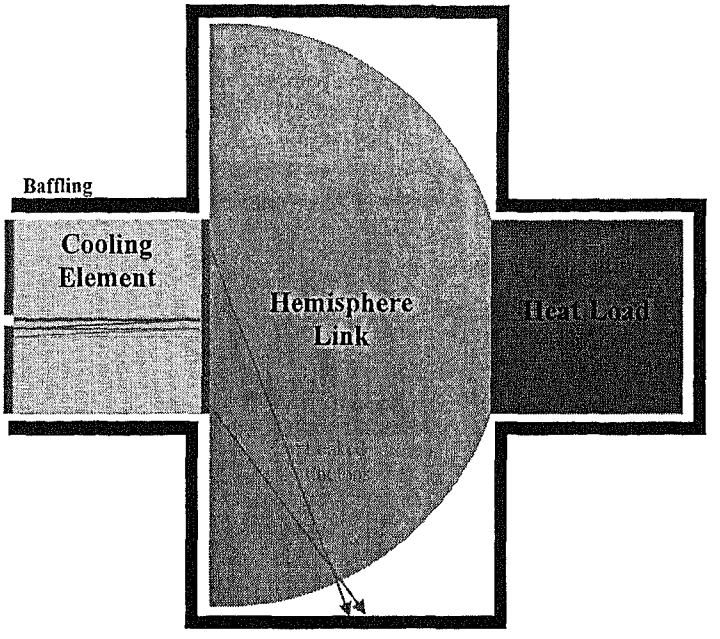

Fig. 5. The hemisphere link design allows all rays to pass through the interface with minimal reflection by keeping the angles of incidence below the critical angle.

2.4 Design 4: Taper

This design uses pyramidal link geometry to decrease the angle of incidence at the vacuum boundary after each internal reflection, taking full advantage of the angular distribution of leaked rays through the dielectric trapping mirrors. As previously discussed, the dielectric mirror on the cooling source leaks almost no light at angles of incidence less than 30°, filtering the angular distribution of light entering the taper. As shown in Fig. 6, the remaining light will undergo a series of internal reflections at the link-vacuum interface. Due to the tapered shape each reflection shifts the direction of light propagation until the light transmits through the sides at near-normal incidence and it is absorbed by the baffling. By the end of the link, the reflected light has become heavily attenuated and the minimal light remaining reflects back towards the cooling element. The length and angle of the taper are adjusted depending on expected mirror leakage and size requirements of the cooling element and heat load.

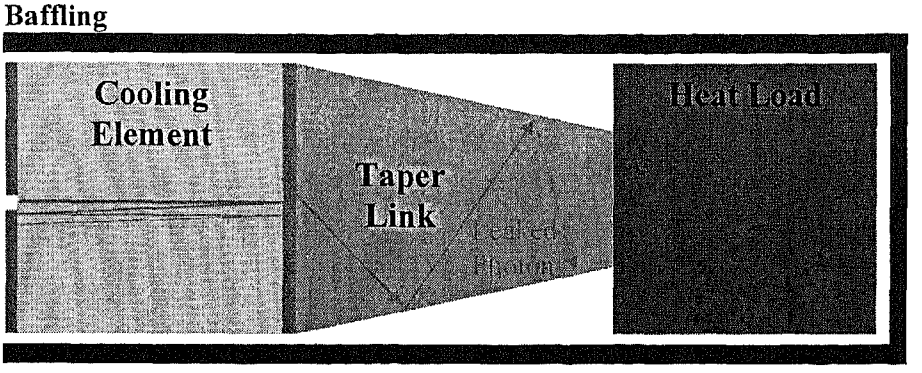

Fig. 6. The figure shows light rays leaked through the mirror and propagating down the link. The link consists of a transparent pyramidal shaped material with a base cross-section area equal to the cooling source which gradually decreases towards the thermal load. As the light rays reflect off the link-vacuum interfaces, the transmission of light increases due to the reflected rays decreased angles of incidence at each bounce.

3. EXPERIMENT

To simplify the tests of our design solutions, we used surrogate materials instead of the specialized doped ZBLANP cooling elements, the high-energy infrared lasers required to observe cooling in a solid, and a complex vacuum chamber setup. As a result we did not observe cooling. Instead, we relied on measurements of light intensity at the location of an absorptive load to calculate the amount of heating that would result from those incident photons. The development of an optical isolation design with the surrogate materials can be translated into the appropriate wavelengths and indices of refraction involved with the actual cooling system by changing material and coating properties. The following subsections describe the approach to creating a light distribution on a 1 cm by 1 cm face that closely resembles the light distribution of that in the LASSOR setup.

3.1 Creation of a wide angular distribution

The surrogate source system is required to mimic the angular distribution caused by uniform fluorescence in the 1 cm^3 cooling source. Several designs were considered, however the most effective surrogate source design scattered light using nanoparticles suspended in a toluene suspension agent inside a 1.2 cm x 1.2 cm x 4.8 cm cuvette. The reasons for choosing this design were to: generate isotropically emitted light by scattering photons in all directions within the cuvette, provide a refractive index close to that of ZBLANP, to provide a constant refractive index within the surrogate source to prevent additional reflections, and to produce a wide angular distribution of light at the outer faces. The use of a scattering solution provided more control over scattering levels than a solid scattering material, and the use of a cuvette provided an ideal surface on which to attach the link designs. A dielectric-mirror-coated microscope slip cover was attached to the emission end of the cuvette with index matching fluid. The mirror was designed to closely match the LASSOR system having high reflectance at near-normal incidence and high transmission at off-normal incidence.

3.2 Suspension agent and cuvette

The small refractive index change between the toluene (n = 1.49) and the cuvette glass (n = 1.52) assured that the wide angular distribution created in the cuvette would not be reduced by refraction. Titanium dioxide nanoparticles have a large refractive index (n = 2.4), which made them highly effective at scattering light when placed in a lower index medium.

The interior cross-section of the cuvette had the same dimensions as the LASSOR cooling source, 1.0 cm x 1.0 cm. The effect of housing the scattering solution within a cuvette resulted in a 1 mm glass separation between the first dielectric mirror material and the scattering solution. This is qualitatively different from the LASSOR setup in which the high

reflectivity coating is applied directly to the glass face. Several of the issues concerning a solution in a cuvette were finite wall thickness, air bubbles, and an elongated axis. The angular distribution of light at the emission face was measured using a photodetector mounted on a radial arm while a hemisphere was optically coupled to the emission face of the cuvette to minimize refraction. The results agreed with the expected values for the angular distribution of light from the LASSOR cooling element.

3.3 Surrogate source setup

Fig. 7 shows the two translators used to adjust the position of the cuvette and the photodetector. The position of the cuvette within the illuminated region was held constant while various link designs were tested. The foam-board was used as highly-absorptive baffling to optically isolate the mirror, thermal link, and photodetector from the light incident upon the cuvette as well as scattered light emitted from other faces. A metal bracket affixed the top of cuvette to the X-Y translator while the bottom of the cuvette rested in a hole in the foam board. The X-Y translator was adjusted to position the emission face of the cuvette parallel to the foam board. The X-Y-Z translator was adjusted to position the photodetector directly at the cuvette emission face. The mirror and thermal link were held between the cuvette and the photodetector by the X-Y-Z translator that was adjusted to apply sufficient pressure to support the link.

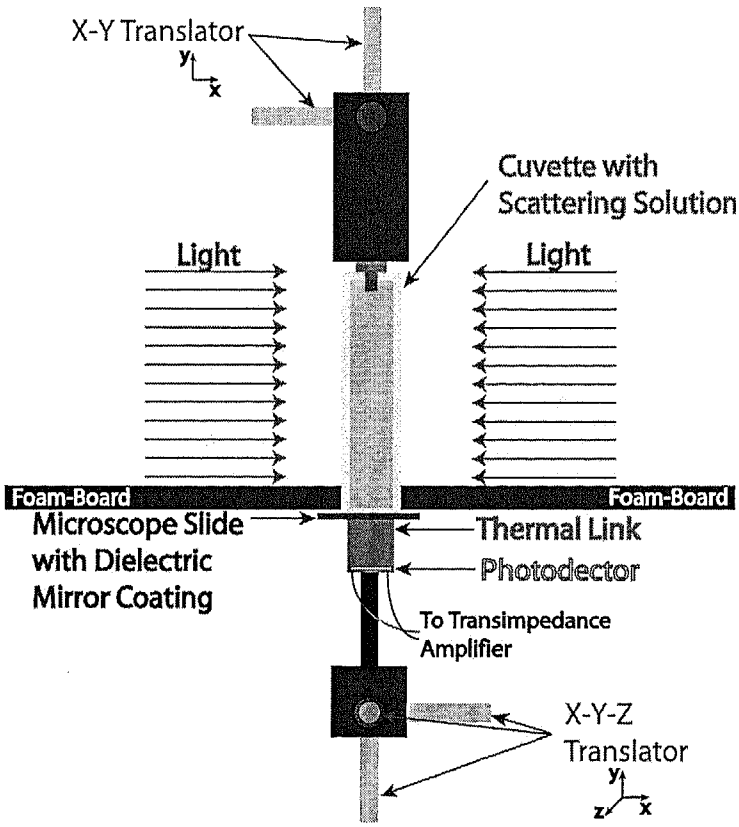

Fig. 7. Surrogate Source Setup (top view)

In order to obtain higher detector sensitivity the team used a lock-in amplifier system, which filtered out the noise and isolated the signal, thereby increasing the signal-to-noise ratio. The modulated signal for the LEDs was generated at 100 Hz to filter-out room lights and was amplified using a Darlington pair current driver. A large active area, 94 mm^2, silicon photodiode was used to capture the transmitted light through the system. The photodiode was optically coupled

to the link to reduce reflections at the interface. The detector's area was equal to that of the expected heat load which provided an effective measure of the total absorbed light at the load.

3.4 Light source

The surrogate system required a light source that provided sufficient power given the sensitivity of the photodetector, but was low enough to be safe to work with. We used light emitting diodes (LEDs) for illumination and worked in the visible spectrum in order to gain immediate visual feedback on the functionality of the link. LEDs provided powerful diffuse illumination at a relatively low cost with a wide variety of visible wavelengths. The surrogate source was pumped with four 627 nm red Luxeon III star LEDs with a spectral half-width of ~30 nm (measured with a grating spectrometer), and a maximum of 210 mW optical power [11]. The half-width of the LED spectrum was characteristic of the LASSOR fluorescence spectrum.

3.5 Dielectric mirrors

Dielectric mirrors were a key component in all of the design solutions. The coated microscope cover slips were ideal for this application given their high reflectivity and low absorption. The ZBLANP cooling element in the LASSOR setup is coated on two opposing faces with dielectric mirrors as a trapping mechanism for the pump laser. The two key characteristics of the cover slip mirrors are their minimal thickness and their refractive index match to the cuvette glass. This allowed us to place the thin mirror against other components in our system using index-matching fluids to reduce interface effects and therefore emulate a coating applied directly. We used No. 1 slip covers with a thickness of 0.13-0.17 mm. We verified the reflection and transmission coefficients of the dielectric mirrors using a He-Ne laser, and by optically coupling the mirror under test between two acrylic hemispheres. We measured the mean mirror intensity reflection coefficient to be .99 from 0° to 40°, which provided a 10° margin on our design estimates by assuming mirror leakage at angles greater than 30°.

3.6 Measurements and verification

The angular distribution of the surrogate source was measured using a pivoting arm with the axis of rotation running through the center of and parallel to the emission face of the cuvette. The photodetector was mounted on the mobile end of the arm facing the emission face. An acrylic hemisphere was placed over the emission face to allow the light to pass through the acrylic interface with minimal refractive effects.

The repeatability of our link transmission results depends on the reproducibility of our angular distribution. The effectiveness of our designs is highly dependent on the angles of light that enter them after leaking through the dielectric mirror. The cuvette emits a large portion of the light distribution in the 50° to 60° leakage angles; however very little light is emitted in the 65° to 75° range. Should the LASSOR system's emission be more heavily weighted towards the 65° to 75° leakage angles, we expect different link transmission results. Based on our calculations and computer modeling, we determined that the surrogate source's angular distribution is a good representation of the LASSOR system, yet the subtle effects of secondary photon absorption and internal reflections could cause deviations in the dominant leakage angles.

4. RESULTS

The designs tested are shown in Fig. 8. Transmission values were calculated using the lock-in amplifier and are shown in Table 1. The two columns of the data represent transmission values with respect to the cuvette face and the mirror face. The transmission from the mirror face provides data that is best suited for comparison with the optical modeling and with similar tests in which the mirror used has a different reflection dependency on angle of incidence.

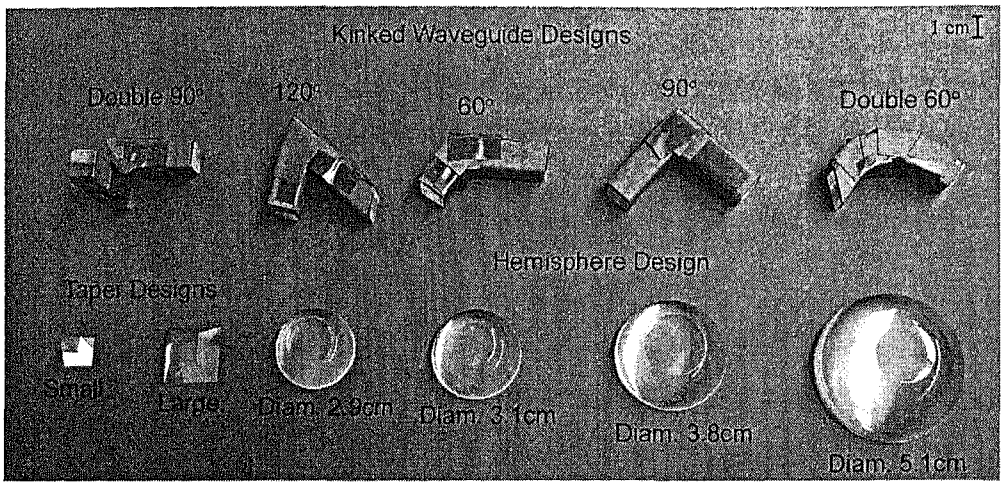

Fig. 8. The photo shows many of the link designs that were fabricated and tested. All designs were created from a single piece of acrylic.

Table 1: Link Transmission Results

Link	Transmission from Cuvette	Transmission from Mirror
Thin 120° KW	0.014±.0003%	0.15±.003%
Small T	0.040±.006%	0.50±.07%
H Diam. 5.1cm	0.049±.006%	0.61±.08%
Double 120° KW	0.071±.007%	0.88±.09%
H Diam. 3.8cm	0.074±.002%	0.92±.03%
H Diam. 3.1cm	0.096±.002%	1.19±.03%
120° KW	0.11±.02%	1.4±.2%
H Diam. 2.9cm	0.122±.004%	1.57±.05%
Double 90° KW	0.32±.006%	3.9±.5%
Large T	0.62±.02%	7.7±.3%
90° KW	1.2±.2%	15±2%
Double 60° KW	1.4±.2%	17±2%
60° KW	1.9±.2%	23±3%
Mirror Alone	8.1±.4%	100%

KW = Kinked Waveguide, H = Hemisphere, T = Taper.

All of the link designs have reduced photon transmission to the thermal load. The most effective link tested was the thin 120° kinked waveguide with a cross-sectional area of 6.25 mm^2, whereas the cross-sectional area of the other kink design was 100 mm^2. However, smaller link cross-sections and longer lengths would further reduce the transmission of light while reducing the rate of heat transfer and increasing black body absorption. To provide a more accurate comparison of the effectiveness of these designs, we only report links that couple to the entire emission face. In this category, the most effect link was the small taper with a net transmission from the cuvette of 0.04%. The net transmission is the most comparable and significant figure for link design evaluation as different mirrors will alter the angular distribution of leaked photons. A link that provides 0.50% transmission of leaked photons from our mirrors will not provide the same transmission with a different dielectric mirror.

As shown in Table 1, the transmission decreased as the size of the hemispheres increased, as the angle of the kink increased, and as the angle of the taper increased – all as expected from theory. The trade-offs between these designs depend on the link volume, the surface area, and the space required inside the LASSOR vacuum chamber. The effects of

these trade-offs on the final load temperature are of a complicated nature and they are the topic of another paper [10]. In addition to these transmission values, results were measured for compound designs achieved by combining multiple systems together. While lower transmission designs were created using such an approach, they are not included here as their sizes became too large to be practical. Future designs to consider might include integrated compound links, which use less material by merging several designs into one piece of acrylic, such as a kinked waveguide with a tapered end. Additional mirrors added before the load and tuned to off-normal incidence would further enhance the link performance.

The links we have tested were made from acrylic. However, sapphire is the link material favored for optical refrigerators as it has a high thermal conductivity, a high transparency to the near IR, and it is well suited for vacuum chamber use. The higher refractive index of sapphire does require a small increase in size from the acrylic link designs.

5. COMPUTER MODEL

For a more rigorous evaluation including Fresnel reflection, Code V optical design software from Optical Research Associates was used to model optical characteristics. The software calculates the behavior of light in an optical system by tracing a large quantity of discreet rays between surfaces in a model and alters the properties of the rays at each surface. Our four designs were modeled as collections of non-sequential surfaces and transmission was analyzed by comparing the optical power exiting the system to the optical power entering the system. With this approach, the effectiveness of the optical isolation of each system was computed.

5.1 Non-Sequential Ray Tracing

As required by the operational requirements of a non-sequential range in Code V, each model consisted of the object (light source), one entrance surface, one exit surface, and the image (where the output intensity is measured). The actual link design was expressed as a non-sequential range of surfaces between the entrance and exit surface. In a totally sequential model, each surface would interact with a ray of light exactly once, yet our Code V model calculated the effects on each ray as it interacted with the surfaces many times, thereby providing an accurate simulation of light reflections in the actual link.

5.2 Surfaces

For each link, the internal side of each surface was specified to be Schott BK7 acrylic material. These calculations did not include the effects of Fresnel reflection, with default surfaces being 100% reflective. In order to correct for this, an acrylic-air dual-layer coating was designed and applied to each surface except for the dielectric mirror. Since multi-layer coatings in Code V do take into account Fresnel reflection, this allowed each surface to perform calculations on each ray that accurately modeled an acrylic-air interface. In order to model the effects of the dielectric mirror, the calculations that Code V performed on rays incident on the mirror were defined manually based on a polynomial fit of the measured angle dependent transmission and reflection properties of the actual mirrors.

5.3 Analysis

The Code V Illumination Option was used to calculate the percentage of power transmitted from the entrance of the link to the exit surface. This option allowed a series of parallel planar sources to be arranged in the shape of a cube at the location of the object to approximate an isotropically emitting volume light source. When a ray is incident on the final (image) surface, at the end of the link, it is terminated and the remaining power is calculated. The program calculates the total power of the all the rays at the final surface, and compares this output power to the initial power to determine the percentage of the light that is attenuated by the link.

5.4 Modeling Results

Table 2 provides a comparison between the Code V optical modeling and the measured results. It is apparent that the computational results vary significantly from the experimentally derived results for each link. This is, however, expected as inherent errors in measuring and applying real data about system components to the models lead to discrepancy between the results. In particular, imperfections in the polynomial fit of the measured angular dependent transmission of the dielectric mirror lead one to expect noticeable deviations between measured and computed values as shown by the 5% transmission difference due to the mirror alone. The angular dependent reflectivity is highly nonlinear which limited the accurate reproducibility of these mirror with an analytic expression. Despite this, the measured and the computed results deviated by less than a factor of three and the ranking of the models has not changed.

Table 2: Computer Modeling Results

Link	Measured Transmission	Computed Transmission
Mirror Alone	8.1%	13%
H Diam. 2.9cm	0.12%	0.35%
H Diam. 5.1cm	0.049%	0.13%
Small T	0.040%	0.033%

6. CONCLUSIONS

We have created a surrogate source to produce an angular distribution of light similar to the fluoresced light from the LASSOR system. Using this surrogate source, we developed methods for testing the effectiveness of thermal links for optical refrigerators with visible light. We have designed, modeled, and tested four of the most promising geometric link designs for preventing the propagation of a wide angular distribution of light. Based on our analysis, we conclude that these link designs will greatly reduce the transmission of photons leading to improved cooling potential for optical refrigerators.

A small taper link design achieved the lowest photon transmission of 0.04% from the source and 0.5% from the mirror, indicating a factor of 200 reduction in light transmission over an optical refrigerator with no link. As colder temperatures are achieved, other heating mechanisms will become significant such as black body radiation and conductive heat transfer through the supporting fibers.

7. ACKNOWLEDGMENTS

This work was performed under a Harvey Mudd College joint Physics-Engineering Clinic project funded by Los Alamos National Laboratory. The authors would like to thank the Los Alamos Solid State Optical Refrigerator team for their helpful insights during this project. The authors are also indebted to Cascade Optical Corporation for their assistance with the dielectric mirror coatings.

REFERENCES

*JJSParker@gmail.com; phone (951) 809-2105

[1] G. Mills, J Fleming, Z. Wei, J Turner-Valle, "Optical cryocooling and the effects of dielectric mirror leakage," NASA ESTO Conf. 2002.

[2] Epstein, R.I., Buchwald, M.I., et al, "Observation of laser-induced cooling in a solid," Nature **377**, 500-502 (1995).

[3] C. Mungan, M. Buchwald, B. Edwards, R. Epstein, "Laser cooling of a solid by 16 K starting from room temperature," Phys. Rev. Let. **78(6)**, 1030-1033 (1997).

[4] R. Epstein, J. Brown. B. Edwards. A Gibbs, "Measurements of optical refrigeration in Ytterbium-doped crystal," J. Appl. Phys. **90(9)**, 4815-4819 (2001).

[5] B. Edwards, J. Anderson, R. Epstein, G. Mills, A. Mord, "Demonstration of a solid-state optical cooler: an approach to cryogenic refrigeration," J. Appl. Phys. **86(11)**, 6489-6493 (1999).

[6] J. Thiede, J. Distel, S. Greenfield, R. Epstein, "Cooling to 208 K by optical refrigeration," Appl. Phys. Lett. **85**, 154107 (2005).

[7] G. Mills, J. Turner-Valle, M. Buchwald, "The first demonstration of an optical refrigerator," AIP Conf. Proc. **710**, 1845-1852 (2004).

[8] G. Mills, W. Good, A. Mord, "The performance of the first optical refrigerator," NASA ESTO Conf. 2004.

[9] G. Mills and A. Mord, "Modeling the performance of an optical refrigerator," NASA ESTO Conf. 2005.

[10] D. Mar, K. Byram, J. Parker et al, "Computer Modeling and Analysis of Thermal Link Performance for an Optical Refrigerator," Photonics West Conf. 2008.

[11] Phillips Lumileds Lighting Company. *Technical Data Sheet DS46.* <http://www.lumileds.com/pdfs/DS46.pdf>